The redundancy and diversity between two novel PKC isotypes that regulate learning in *Caenorhabditis elegans*

Shingo Hiroki[a] **and Yuichi Iino**[a,1]

[a]Department of Biological Sciences, Graduate School of Science, The University of Tokyo, Tokyo 113-0033, Japan

Edited by Paul Sternberg, Division of Biology and Biological Engineering, California Institute of Technology, Pasadena, CA; received April 14, 2021; accepted November 16, 2021

The nematode *Caenorhabditis elegans* learns the concentration of NaCl and moves toward the previously experienced concentration. In this behavior, the history of NaCl concentration change is reflected in the level of diacylglycerol and the activity of protein kinase C, PKC-1, in the gustatory sensory neuron ASER and determines the direction of migration. Here, through a genetic screen, we found that the activation of Gq protein compensates for the behavioral defect of the loss-of-function mutant of *pkc-1*. We found that Gq activation results in hyperproduction of diacylglycerol in ASER sensory neuron, which leads to recruitment of TPA-1, an nPKC isotype closely related to PKC-1. Unlike the *pkc-1* mutants, loss of *tpa-1* did not obviously affect migration directions in the conventional learning assay. This difference was suggested to be due to cooperative functions of the C1 and C2-like domains of the nPKC isotypes. Furthermore, we investigated how the compensatory capability of *tpa-1* contributes to learning and found that learning was less robust in the context of cognitive decline or environmental perturbation in *tpa-1* mutants. These results highlight how two nPKC isotypes contribute to the learning system.

Caenorhabditis elegans | learning | genetics | PKC | isotypes

Diacylglycerol (DAG) and its major target, protein kinase C (PKC), are key molecules in various biological processes (1, 2). In the nervous system, this signaling pathway functions in diverse events of information processing, including response to neurotransmitters (3), synaptic vesicle release (4), nociception (5, 6), and, most notably, learning (7–9).

PKC can be divided into three subclasses: conventional PKC (cPKC), novel PKC (nPKC), and atypical PKC (aPKC). Each PKC requires distinct upstream activators. Specifically, cPKC is activated by Ca^{2+} and DAG, nPKC is activated by DAG, and aPKC responds to neither DAG nor Ca^{2+}. Furthermore, each subclass includes several isotypes: In mammals, PKC-α, PKC-β, and PKC-γ belong to cPKC. PKC-ε, PKC-η, PKC-δ, and PKC-θ belong to nPKC, while PKC-ζ and PKC-ι belong to aPKC (10). These diverse isotypes can function similarly (11, 12) or in a distinct manner (8, 10), suggesting that there are both differences and redundancies between PKC isotypes. However, how the redundancies and differences between these isotypes contribute to biological functions is an elusive question, especially in the nervous system. Previous studies using knockout mutants or pharmacological activation revealed the contribution of each PKC to behavior. Nevertheless, since the nervous system has a highly heterogeneous nature and PKCs are expressed in diversely overlapping patterns, it is difficult to attribute these behavioral consequences to the function of each isotype.

Functions of PKCs are well studied in the nematode *Caenorhabditis elegans* (13). Since the nervous system of *C. elegans* consists of a limited number of neurons (about 300), the function in certain neurons can be studied by cell-specific manipulation of each PKC (14–17). Several studies have shown that *C. elegans* uses DAG/PKC as a canonical signaling pathway to memorize environmental NaCl concentration in the gustatory sensory neuron ASER: when *C. elegans* is conditioned at a certain concentration of NaCl in the cultivation medium, it migrates toward that concentration on an NaCl gradient (18–20). In this type of learning, changes in ambient NaCl concentration are represented by the abundance of DAG in the gustatory sensory neuron ASER (19): decrease in NaCl concentration activates ASER and causes an increased $[Ca^{2+}]$ in ASER, which results in an increase of DAG through the activation of EGL-8/PLC-beta. Conversely, an increase in salt concentration causes the opposite event, leading to a decrease of DAG. Furthermore, when PKC-1, an isotype of nPKC, is activated in ASER by DAG, the animals climb up the NaCl gradient, and when PKC-1 is inactivated, they descend down the gradient.

To look more closely into the mechanism, we performed genetic screening to obtain a suppressor mutant of *pkc-1(nj3lf, loss of function)*. Interestingly, we found that activation of the Gq protein, which is considered to act upstream of DAG production, compensates for loss of *pkc-1*. Further analysis revealed that Gq functions in ASER to elevate the amount of DAG and thereby activates TPA-1, an nPKC isotype closely related to PKC-1. As a result, TPA-1 compensates for PKC-1 downstream of Gq. However, despite the compensatory capability of TPA-1, the *tpa-1* mutant did not show any obvious defect in learned behaviors. This difference in the phenotypes between the nPKC mutants was suggested to be due to differences in their sensitivity to DAG, because TPA-1 seemed to

Significance

The nervous system can store an experience of sensory stimulus. This function (i.e., learning) requires a robust molecular mechanism because accurate readout of information is crucial in survival. In this study, we found that the gustatory learning of *Caenorhabditis elegans* implemented as the amount of diacylglycerol in the sensory neuron can be read out not only by the activity of PKC-1, a protein kinase C, but also by that of another PKC, TPA-1. Because of its low sensitivity to diacylglycerol, TPA-1 does not function in the conventional learning assay. However, under conditions that may impair the system, such as aging, TPA-1 contributes to the learning. Our study shows the robustness of the learning system achieved by the two PKCs.

Author contributions: S.H. designed and performed research, contributed new reagents/analytic tools, and analyzed data; and S.H. and Y.I. wrote the paper.

The authors declare no competing interest.

This article is a PNAS Direct Submission.

[1]To whom correspondence may be addressed. Email: iino@bs.s.u-tokyo.ac.jp.

This article contains supporting information online at http://www.pnas.org/lookup/suppl/doi:10.1073/pnas.2106974119/-/DCSupplemental.

Published January 13, 2022.

respond only to higher concentration of DAG to generate migration bias. The expression of domain-replaced *tpa-1* suggested that this difference in sensitivity arose from the difference in the C1 and C2-like domains. Furthermore, we sought to reveal how compensatory capability and redundant function of *tpa-1* contribute to learning. We found that *tpa-1* mutants show an impaired learning in the contexts of aging and multisensory perturbation. The former phenotype was rescued by the expression of *tpa-1* in ASER, while the latter was not.

These results suggest that *tpa-1* is dispensable in the conventional chemotaxis assay due to its lower sensitivity, while it still has supportive function in various contexts including aging.

Results

Go Inactivation and Gq Activation Compensate for the Impaired Migrational Bias in NaCl Chemotaxis of the *pkc-1* Mutant. *C. elegans* is known to exhibit chemotaxis toward the salt concentration at which they were cultivated (18–20). To evaluate this type of learning ability, we used the established behavioral assay (Fig. 1*A*) (18); worms were conditioned at 25 mM, 50 mM, or 100 mM and placed on 9-cm plates with a salt gradient from ∼35 mM to ∼95 mM. Migration bias was quantified using the chemotaxis index (see *Methods* for definition). In this assay, as previously reported (18), *pkc-1(nj3lf)* mutants always migrated toward low salt concentrations regardless of the cultivation conditions (Fig. 1*B*). To identify mutations that suppress the abnormal migration bias of *pkc-1*, we mutagenized the *pkc-1(nj3lf)* mutant using ethyl methanesulfonate (EMS) and performed a forward genetic suppressor screening (see *Methods*). Among the obtained mutants, we found that a mutation in the N-terminal region of *goa-1*, His322Tyr, partially suppressed *pkc-1(nj3)* (Fig. 1*B* and *SI Appendix*, Fig. S1).

It is known that *goa-1* encodes the alpha subunit of the trimeric G protein, Go. It often functions by antagonizing the Gq pathway in *C. elegans* (21). Therefore, we examined whether the mutation *pe914[Y61N]gf*, a constitutively active mutation of the Gαq homolog *egl-30* (22), would also compensate for *pkc-1(nj3)*. The results showed that *egl-30(pe914gf)* can also suppress *pkc-1(nj3lf)* (Fig. 1*C*), indicating that activation of Gq compensates for the loss of *pkc-1(lf)* in the learned behavior.

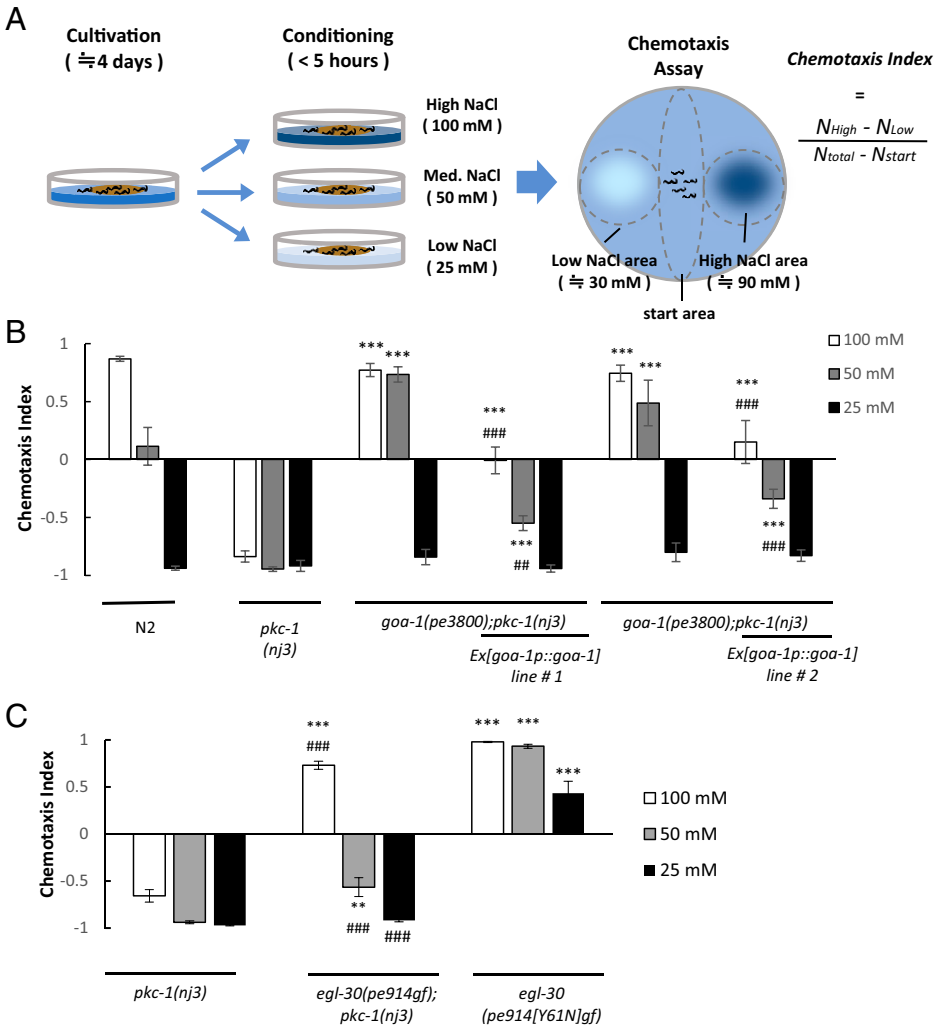

Fig 1. Inactivation of Go and activation of Gq compensate for the migrational bias in NaCl chemotaxis of the *pkc-1(lf)* mutant. (*A*) Schematic diagram of salt-chemotaxis learning in *C. elegans*. Animals were conditioned on NGM plates with high (100 mM), intermediate (50 mM), or low (25 mM) concentration of NaCl. After 5 or fewer hours, they were placed on an assay plate with the NaCl gradient. (*B*) *goa-1(pe3800[H322Y])* suppresses migration bias of *pkc-1(nj3lf)*. Chemotaxis in wild type is shown in the left panel. The color of each bar represents the concentration of NaCl in conditioning plates (indicated on the right end of the graph). Error bars indicate SEM; $n = 6$ assays. *P* values were determined by ANOVA followed by Tukey's test for comparison of each strain conditioned by the same concentration. ***$P < 0.001$ for the comparison to *pkc-1(nj3)*. ###$P < 0.001$, ##$P < 0.01$ for the comparison to *goa-1(pe3800);pkc-1(nj3)*. (*C*) *egl-30(pe914[Y61N]gf)* also suppresses *pkc-1*. $n = 6$ assays. **$P < 0.01$, ***$P < 0.001$ for the comparison to *pkc-1(nj3)* and ###$P <$ 0.001 for the comparison to *egl-30(pe914)* in Tukey's test.

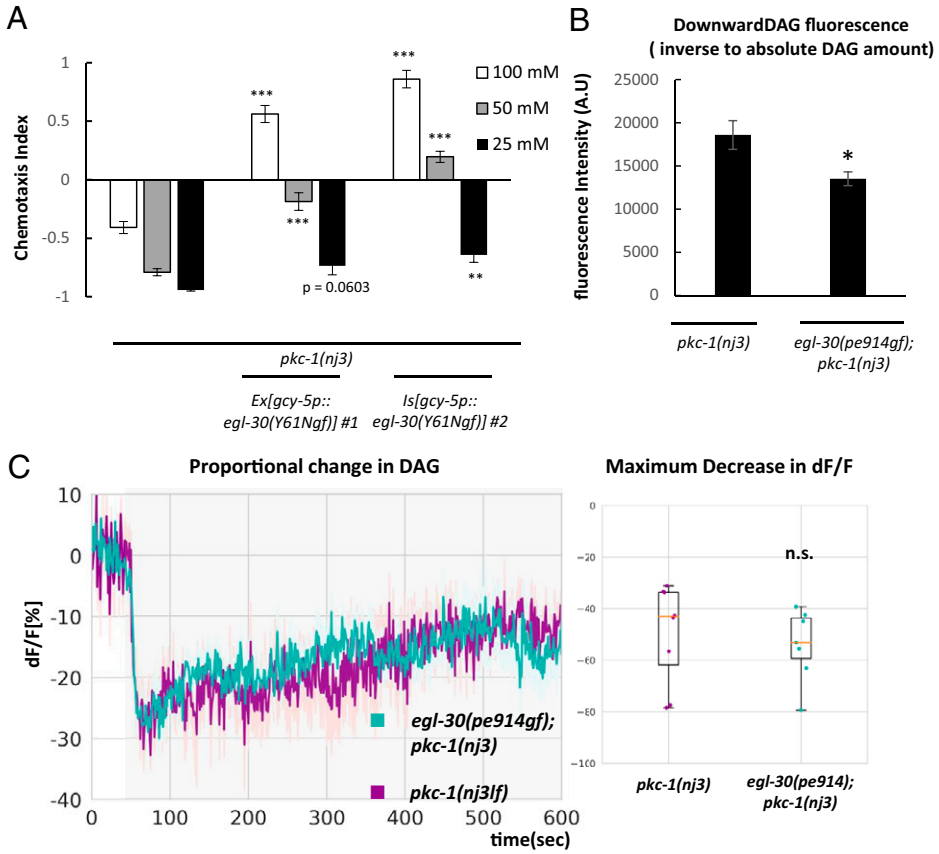

Fig. 2. Activated Gq/*egl-30* functions in ASER to promote DAG production. (*A*) Chemotaxis of *pkc-1(nj3)* mutants expressing *egl-30(Y61Ngf)* under the ASER-specific *gcy-5* promoter. $n = 6$ assays (line #1) or 5 assays (line #2), respectively. *P* values were determined by Dunnet's test. $^{**}P < 0.01$, $^{***}P < 0.001$. Note that the transgene in line #2 was spontaneously integrated during isolation. (*B*) The effect of *egl-30(pe914gf)* on the basal DAG levels in ASER. Downward DAG2, an inverse-type fluorescent reporter of DAG, was expressed in ASER. Error bar indicates SEM. $n = 13$ animals (*nj3*) and 14 animals(*pe914;nj3*), respectively. *P* values were determined by Welch's test. $^{*}P < 0.05$. (*C*) The effect of *egl-30(pe914gf)* on DAG changes induced by NaCl decrease. Animals were conditioned with 100 mM NaCl and then transferred to microfluidic chip filled with imaging buffer containing 100 mM NaCl. A decrease in NaCl (100 to 50 mM, gray shed) was applied 50 s after the start of image acquisition. dF/F indicates change in fluorescence relative to intial fluorescence (F0, see *Methods*). Note that a Downward DAG2 is an inverse-type probe; therefore, a decrease in fluorescence is interpreted as an increase in the amount of DAG. $n = 7$ animals (*nj3*) and 8 animals (*pe914;nj3*), respectively. *P* values were determined by Welch's test. n.s., not significant ($P > 0.05$).

Activation of Gq in ASER Compensates for the Chemotaxis Defect of *pkc-1* Mutants. Next, we sought neurons in which *egl-30(gf)* functions. Because *pkc-1* functions in ASER (18), we first tested whether ASER-specific expression of *egl-30(gf)* would also compensate for *pkc-1(nj3)*. We found that *egl-30(gf)* functions in ASER, the same site as *pkc-1* (Fig. 2*A*). This was intriguing, since Gq activation generally transduces a signal by activating PLC-beta and thereby producing DAG. To further investigate the function of *egl-30* in ASER, we performed DAG imaging using the inverse-type fluorescence probe Downward DAG2 (19, 23). Indeed, *egl-30(gf)* increased the basal (i.e., the absolute amount) DAG level in ASER (Fig. 2*B*). On the other hand, the proportion of increase in DAG amount induced by an NaCl decrease was not altered in *egl-30(gf)* (Fig. 2*C*), suggesting that the *egl-30(gf); pkc-1(lf)* mutant maintains a higher DAG amount compared to *pkc-1(lf)* even when they are subjected to any salt-concentration changes during the learning assay. This can explain the high-salt migration phenotype of *egl-30(gf)*, which is similar to the behavior caused by chronic addition of DAG analog, phorbol ester, to wild type (ref. 18, Fig. 3D).

These results suggest that Gq activation changes the salt-concentration preference through increase in the amount of DAG, which can activate PKC. Indeed, the phenotype of *egl-30(pe914gf); pkc-1(lf)* double mutant was significantly different from that of *egl-30(pe914gf)* (Fig. 1*C*), indicating that *egl-30(pe914gf)* is suppressed by *pkc-1(lf)* (mutual suppression). However, the suppression was partial, suggesting that factors other than PKC-1 function downstream of DAG.

TPA-1, a DAG-Dependent and Ca^{2+}-Independent PKC, Acts downstream of Gq to Compensate for the Loss of PKC-1. Next, we searched for other genes that function downstream of Gq. Apart from PKC-1, there is another PKC isotype called TPA-1 (13, 24). As predicted, the phenotype of the triple mutant demonstrated that *tpa-1(fr1lf)* strongly suppressed the effects of *egl-30(gf)* in the *pkc-1(lf)* background (Fig. 3*A*). Furthermore, the effects of *tpa-1(fr1)* were cancelled by the expression of wild-type *tpa-1* in ASER (Fig. 3*C*). These results suggest that *tpa-1* acts downstream of activated Gq in ASER and thus compensates for the low-salt chemotaxis bias caused by the loss of *pkc-1*. However, while *tpa-1* seems to have a compensatory function in chemotaxis, the *tpa-1(fr1)* single mutant did not show any obvious abnormalities in chemotaxis (Fig. 3*B*). This suggests that *tpa-1* has some characteristics that are different from *pkc-1*, which may prevent *tpa-1* from affecting PKC-1–mediated transduction of DAG abundance.

Functional Diversity between PKC-1 and TPA-1. Based on the known molecular mechanisms of Gq activation, we hypothesized that TPA-1 may only respond to high levels of DAG. To test this, we treated

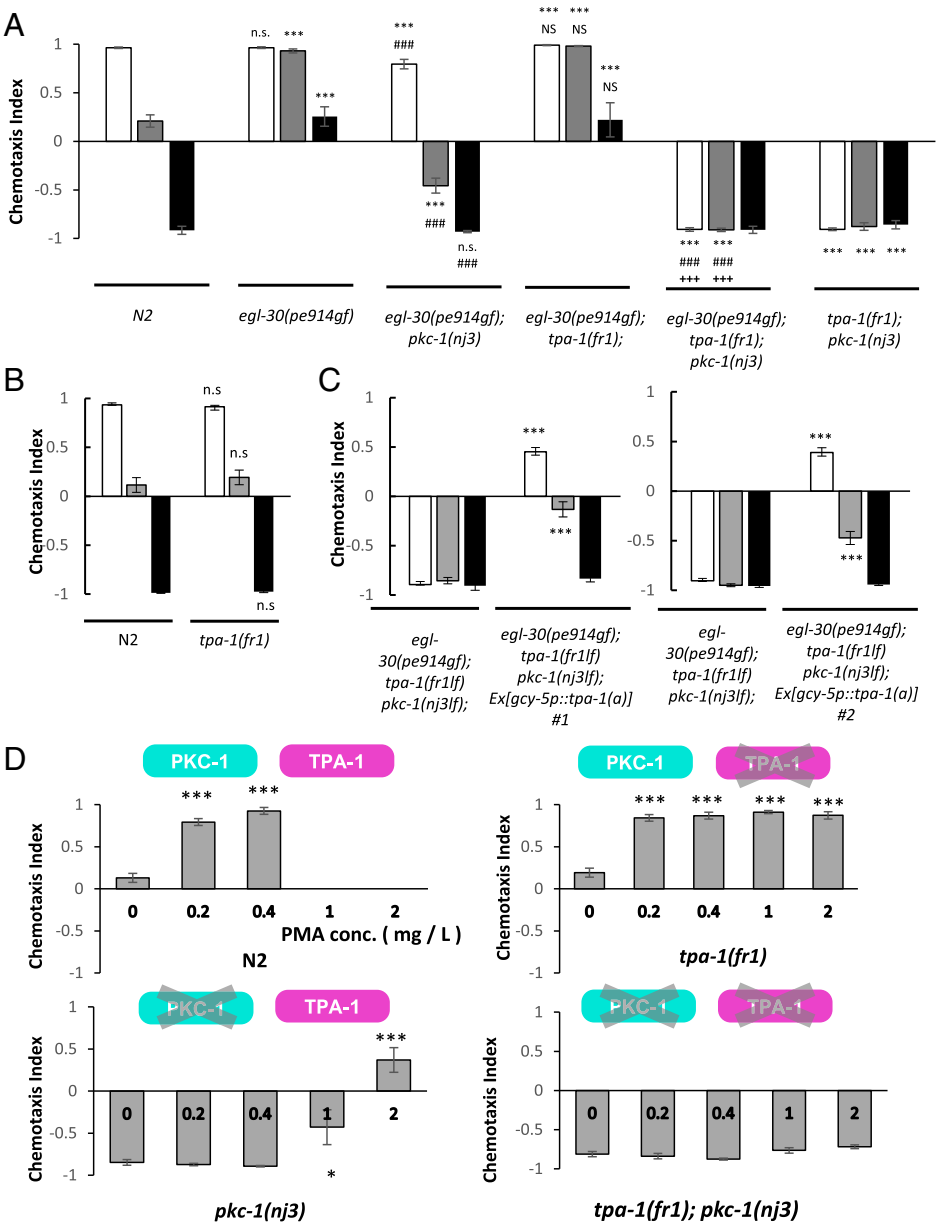

Fig. 3. TPA-1 functions downstream of *egl-30(gf)* to compensate for loss of *pkc-1*. (*A*) The *tpa-1(fr1)* mutation suppresses the compensatory effect of *egl-30(pe914)* in *pkc-1(nj3)* mutants. $n = 6$ assays. *P* values were determined by Tukey's test. n.s., $P > 0.05$, $^{***}P < 0.001$ compared to N2. NS, $P > 0.05$, $^{\#\#\#}P < 0.001$ compared to *egl-30(pe914)*. $^{+++}P < 0.001$ compared to *egl-30(pe914);pkc-1(nj3)*. (*B*) Chemotaxis of *tpa-1(fr1)* mutants. $n = 6$ assays. *P* values were determined by Welch's test. n.s., not significant ($P > 0.05$). (*C*) Suppression by *tpa-1(fr1)* was rescued by expression of wild-type *tpa-1* under the *gcy-5* promoter. *P* values were determined by Welch's test. $n = 7$ to 8 assays. $^{***}P < 0.001$. (*D*) The dose-dependent effect of the DAG analog PMA in nPKC mutants. Animals were conditioned with NGM plates containing 50 mM NaCl and indicated concentrations of PMA. As described in the illustrations, *pkc-1(nj3)* mutants, which have functional *tpa-1* but not *pkc-1*, showed chemotactic bias only when treated with high (>1.0 μg/mL) concentrations of PMA. *P* values were determined by Dunnett's test. $n = 6$ assays. $^{*}P < 0.05$,$^{**}P < 0.01$, $^{***}P < 0.001$ for comparison to 0 mg/mL PMA.

mutants with different concentrations of Phorbol 12-myristate 13-acetate (PMA), a potent DAG analog. When treated at 0.2 to 0.4 mg/mL, wild-type *C. elegans* showed a chemotaxis bias in the direction of high-salt concentration (Fig. 3*D*). As shown in previous studies (25, 26), motility was strongly inhibited by PMA at or above 1 mg/mL, preventing the measurement of chemotaxis. In turn, *tpa-1(fr1)* mutants did not show abnormalities in motility when exposed to high concentrations of PMA (25), whereas a chemotaxis bias to high-salt concentrations was induced by all concentrations of PMA at or above 0.2 mg/mL. Importantly, *pkc-1(nj3)* did not alter chemotaxis upon application of low concentrations of PMA, whereas chemotaxis shifted in the direction of high-salt concentrations when exposed to high concentrations of PMA at or above 1 mg/L. Furthermore, the effect of PMA was negligible in the *pkc-1(nj3); tpa-1(nj3)* double mutant. These results suggest that TPA-1 responds to a higher concentration of DAG than PKC-1 does.

To explore which molecular differences cause functional differences between TPA-1 and PKC-1, we examined whether we could rescue *pkc-1(nj3)* by expressing *tpa-1*, whose domain was replaced with that of *pkc-1*. Here, we focused on three major domains: C2-like, C1, and kinase domains. First, we expressed wild-type *pkc-1* or *tpa-1* in the ASER of the *pkc-1(nj3)* mutant. While expression of *pkc-1* clearly rescued the phenotype, the expression of *tpa-1* had little effect on chemotaxis (Fig. 4 *A* and

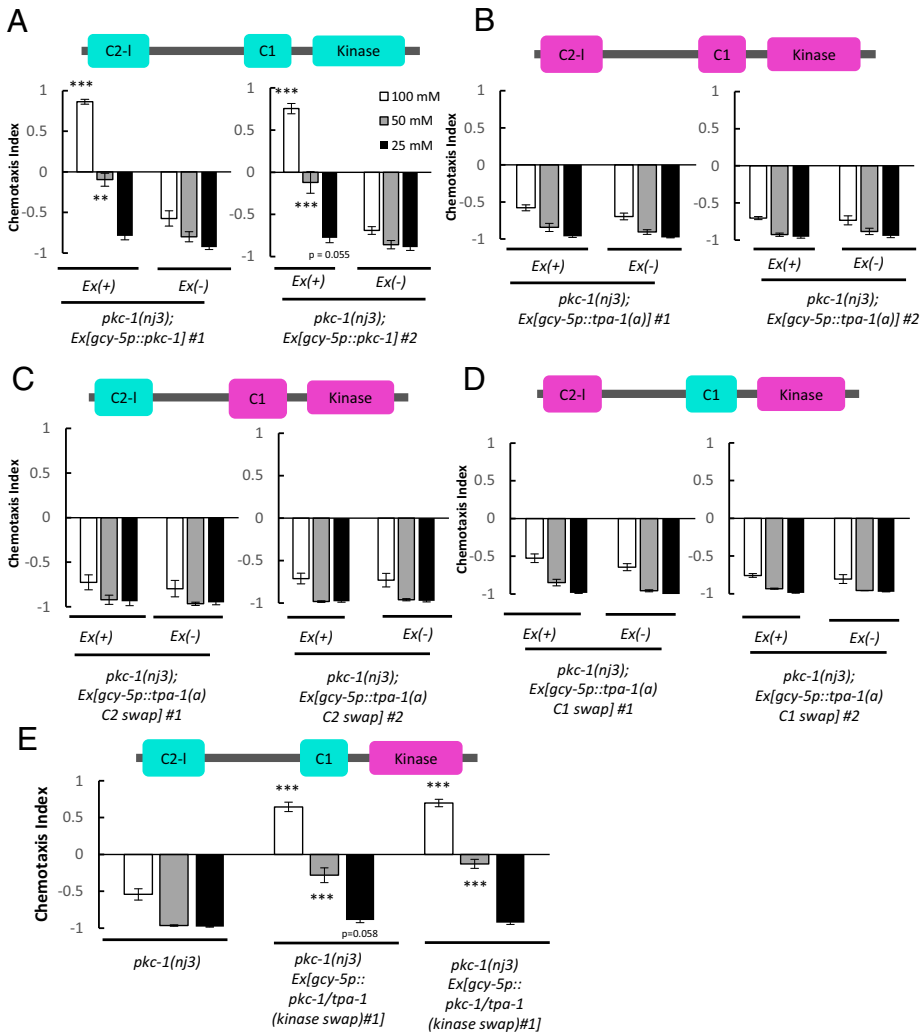

Fig. 4. The effect of expression of chimeric genes of TPA-1 and PKC-1. (*A*) The effect of the expression of wild-type *pkc-1* on chemotaxis in the *pkc-1* mutant. $n = 6$ assays. (*B*) The effect of expression of wild-type *tpa-1* in the *pkc-1* mutant. Each transgenic line was generated by outcrossing *egl-30(pe914);tpa-1(fr1);pkc-1(nj3);Ex[gcy-5p::tpa-1]* in Fig. 3*C*; thus, the transgenic arrays must have an ability to rescue the phenotype of the triple mutant. $n = 6$ assays. (*C*) The effect of the expression of chimeric *tpa-1* on chemotaxis, whose C2-containing sequence was replaced with that of *pkc-1* in *pkc-1(nj3)* mutants. (*D*) Effect of the expression of chimeric *tpa-1* on chemotaxis, whose C1-containing sequence was replaced with that of *pkc-1* in *pkc-1(nj3)* mutants. $n = 6$. For *A*–*D*, *P* values were determined by Welch's test. $^{***}P < 0.001$, $^{**}P < 0.01$. (*E*) The effect of the expression of chimeric *tpa-1* on chemotaxis, whose C1- and C2-containing sequences were replaced with those of *pkc-1* in *pkc-1(nj3)* mutants. $n = 7$ assays. *P* values were determined by Dunnet's test for comparison of each strain conditioned by the same concentration. $^{***}P < 0.001$ for the comparison to *pkc-1(nj3)*.

B). This confirms the functional difference between the two nPKCs. Next, we expressed *tpa-1* whose C1 or C2-like domain was replaced with the corresponding domain of *pkc-1*. No effect was observed in either case (Fig. 4 *C* and *D*). In contrast, when both C1 and C2-like domains were replaced, the chemotaxis of *pkc-1* mutants was clearly rescued (Fig. 4*E*). This suggests that the cooperative activity of the C1 and C2-like domains is responsible for the difference in responsiveness between PKC-1 and TPA-1.

These results suggest that differences in both C1 and C2-like domains lead to higher DAG sensitivity of PKC-1 compared with TPA-1; therefore, TPA-1 does not to show a significant function in our standard chemotaxis assay.

TPA-1 Contributes to Robustness of Learned Behaviors in the Context of Aging or Environmental Perturbation. These results indicate that the nPKC isotypes PKC-1 and TPA-1 carry overlapping potentials, but in the absence of *pkc-1*, *tpa-1* cannot replace *pkc-1* under standard conditions. Then what is the biological significance of the compensatory capability of *tpa-1* in chemotaxis? Because redundancy is generally considered to contribute to robustness of a system, we focused on the robustness of learning in the *tpa-1* mutant. Inspired from a previous study, which reported that activation of Gq slows the aging-dependent decline of long-term memory in olfactory associative learning (27), we inspected whether loss of DAG/PKC component, TPA-1, might result in learning impairment in aged worms. Indeed, the ability of salt-concentration learning gradually declined in wild type with aging (*SI Appendix*, Fig. S3). In contrast to typical chemotaxis assays with young adult worms (days 0 to 1), aged (day 4) *tpa-1* worms showed a significant impairment in learning when conditioned with high NaCl (Fig. 5*A*). This was rescued by the expression of *tpa-1* in ASER, indicating that functional redundancy indeed contributes to the robustness of learning.

Furthermore, we tested whether *tpa-1* contributes to robustness of learning under environmental perturbation. A recent study demonstrated that ASER is a polymodal neuron that perceives

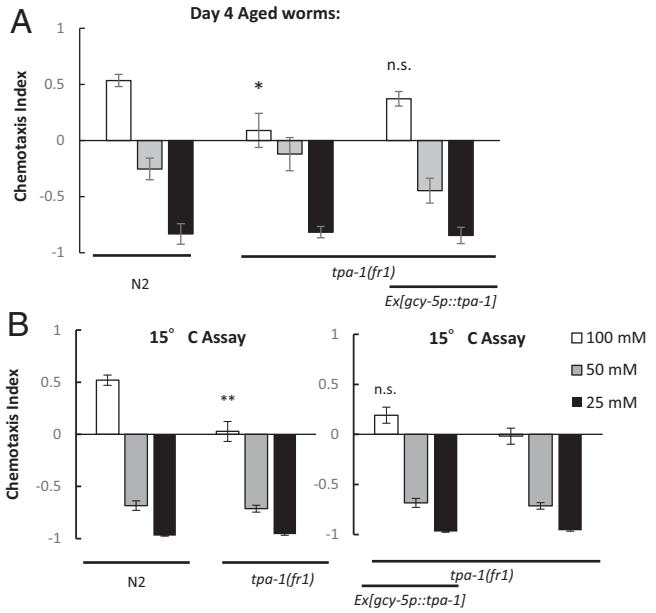

Fig. 5. *tpa-1* contributes to memory robustness. (*A*) Chemotaxis in the aged worms. *tpa-1(fr1);Ex[gcy-5p::tpa-1]* was generated by outcrossing *egl-30(pe914);tpa-1(fr1);pkc-1(nj3);Ex[gcy-5p::tpa-1]* line #1 in Fig. 3*C*. $n = 6$ assays. *P* values were determined by Dunnet's test for comparison of each strain conditioned by the same concentration. n.s., $P > 0.05$, $^{*}P < 0.05$ for the comparison to N2. (*B*) The effect of temperature transfer in wild type and *tpa-1(fr1)* mutants. *tpa-1(fr1);Ex[gcy-5p::tpa-1]* is the same transgenic line as panel *A*. $n = 7$ assays(N2), 8 assays (*fr1, fr1;Ex[gcy-5p::tpa-1]*). *P* values were determined by Welch's test. n.s., $P > 0.05$, $^{**}P < 0.01$ compared to N2 (*left*) or Ex(-) (*right*).

cold temperatures via *goa-1* (28). This led us to investigate whether temperature change would perturb salt-concentration learning. To test this, we conditioned worms at room temperature and performed the chemotaxis assay in a cold environment (at 15 °C, Fig. 5*B*). Wild-type worms conditioned at 50 mM NaCl showed chemotaxis toward low concentration, showing remarkable impairment in learning. On the other hand, the learning at 100-mM conditioning showed a certain degree of tolerance. The *tpa-1(fr1)* mutant, in turn, was less tolerant to perturbation (Fig. 5 *B*, *left*). However, this defect was not rescued by the expression of *tpa-1* in ASER (Fig. 5 *B*, *right*). As such, *tpa-1* may function in cells other than ASER for this function. Likewise, we also tested the sustainability of memory by setting a prolonged posttraining period (*SI Appendix*, Fig. S2), showing that *tpa-1* also contributes to the sustainability of memory by acting in neurons other than ASER.

Taken together, these results show that *tpa-1* contributes to robustness of learning in ASER and other neurons.

Discussion

PKC-1 and TPA-1 Work Partially Redundantly. In this study, we found that Gq activation and high levels of DAG abundance recruit *tpa-1* to compensate for the loss of *pkc-1* (Figs. 1*B* and 3*A*). Most previous reports have focused on different phenotypes for each mutant. For instance, *tpa-1* mutants show impaired innate immune response, while *pkc-1* mutants do not (29). Also, *pkc-1* mutants show defects in tap response habituation, while *tpa-1* mutants do not (30). Another study showed redundant functions of *tpa-1* and *pkc-1* in PMA-mediated enhancement of odor chemotaxis (16, 31). Our data indicate that *pkc-1* and *tpa-1* have redundant functions but have differential responsiveness to DAG.

The mammalian homologs of PKC-1 and TPA-1, PKC epsilon and PKC delta, are also known to function differently (32) or even oppositely (33), while another report suggests that they function redundantly (12). It will be worth examining whether these PKCs also have functional difference and redundancy in the nervous system, as observed in this study.

C1 and C2-like Domains Cause the Difference between PKC-1 and TPA-1. Our data suggest that a DAG-binding domain, C1 domain, functions cooperatively with the C2-like domain to cause a difference between PKC-1 and TPA-1. Unlike the C2 domain of conventional PKCs, C2-like domains of nPKCs do not bind to Ca^{2+}. On the other hand, C2-like domains play an important role in interactions with lipids or the C1 domain (34, 35). Furthermore, a large conformational difference is known to exist between the C2-like domain of PKC epsilon and that of PKC delta, which results in a difference in their binding capacities (34, 36). Our study suggests that the functional consequence of diversity in the C1 and C2-like domains may provide a strategy for designing specific inhibitors or activators of each PKC isotype.

tpa-1 Functions against Cognitive Decline. Fig. 5*A* indicated the function of TPA-1 in aged worms. The DAG level might be high enough to at least partially activate TPA-1 when transferred from the 100-mM conditioning plate. This appears to be consistent with the phenotype of *pkc-1(nj3)*, which occasionally shows a higher chemotaxis index in 100-mM conditioning compared to 25-mM conditioning, possibly by the function of TPA-1 (see Figs. 2*A* or 3 *B* and C, for example). In aged nematodes, the activity of PKC-1 is probably reduced, and TPA-1 likely compensates for the reduction of the activity. In mammals, the activities of PKCs are considered to decline with aging. Intriguingly, in the hippocampus, the function of PKC epsilon (37, 38), the PKC-1 homolog, is significantly reduced with aging, while that of PKC delta, the TPA-1 homolog, remains unchanged (37). Therefore, PKC delta might also function in cognitive decline in a similar way to TPA-1. If the function of PKC-1 declines with aging progression like PKC epsilon in mammals, TPA-1 might work instead of PKC-1.

Partial Redundancy Makes a Robust System. In addition to the conditions we tested in this study, there could be multiple factors that lead to the modulation or dysfunction of PKC-1. This could be a general problem that signaling pathways such as DAG/PKC-1 may often face. In the case of a digital signaling system, in which there are quasibinary changes in the second messengers, such as the cellular response to rapid changes in the external ligand, the robustness of the system can be ensured simply by having multiple functionally equivalent kinases. On the other hand, in an analog system, such as the DAG/PKC coding system for salt chemotaxis, in which the strength of the signal must be precisely encoded, even if there are multiple kinases that are functionally identical, the total amount of phosphorylation as an output cannot be properly controlled; if the activity of one of the kinases is reduced, the total amount of output will change when the amount of DAG is not sufficient to fully phosphorylate the substrates. If there are two kinases, one of which having lower sensitivity, the dysfunction of the less sensitive kinase would not impact the total output because the phosphorylation of the substrates might be nearly saturated. In addition, when the other kinase is somewhat functionally declined, the less sensitive kinase can compensate for it if the amount of DAG is sufficient. Our results suggest that in such an analog system, the robustness of the system can be achieved by including redundant molecules with different sensitivities to the second messengers.

Methods

***C. elegans* Strains and Culture.** The list of strains used in the experiments is shown in *SI Appendix*, Table 1. All mutants were outcrossed at least five times. Wild-type animals corresponded to the Bristol strain N2. Animals were maintained at 20 °C on the nematode growth media (NGM) plate, unless otherwise noted (39). Day 4–aged worms were age-synchronized by bleaching. After they were sexually matured (4 d after bleaching, day-0 adults), we washed the worms with the wash buffer every other day to avoid contamination of progeny. We performed chemotaxis assays after 4 d.

For behavioral assays, the animals were fed with *Escherichia coli* NA22 bacteria. For imaging experiments, they were fed with OP50 to avoid noise from autofluorescence of the intestine.

Behavioral Tests. Salt chemotaxis assays were performed as previously described with slight modifications (18). Briefly, NaCl gradients were generated on assay plates with 9 cm diameter by placing two agar plugs (cylinder, 14.5 mm in diameter, with 150 mM and 0 mM NaCl) 23 to 25 h before the assay. Adult animals were washed from the growth plate and conditioned on NGM plates at certain concentrations (25 mM, 50 mM, and 100 mM) of NaCl. After 5 to 7 h of conditioning, they were collected from conditioning plates, washed two times to remove bacteria, and then placed onto the assay plates with NaCl gradient. Just before the assay, agar plugs were removed and, in turn, 1 μL 0.5 M NaN_3 was spotted at the position of each agar plug. The animals were allowed to run on the plates for ∼60 min. Then, animals were immobilized by transferring plates to 4 °C. For the quantification of chemotaxis, we counted the number of worms in each region described in Fig. 1*A*. The chemotaxis index is calculated as $(N_{high\text{-}salt} - N_{low\text{-}salt})/(N_{all} - N_{start\ point})$.

For PMA treatment, plates with each concentration of PMA were prepared by adding 10 mg/mL PMA in EtOH to NGM before pouring into plates.

Molecular Biology and Transformation. Gateway technology (Invitrogen) was used to generate cell-specific expression plasmids; for ASER-specific expression, the *gcy-5* promoter (3.2 kb upstream), which was cloned into the pENTR vector, was used. To clone complementary DNA (cDNA) or generate chimeric cDNA, we used the In-Fusion HD Cloning Kit (Takara).These were cloned into pDEST vectors. *goa-1*p::*goa-1* and *gcy-5p::egl-30(Y61Ngf)* were the same plasmids as previously described (22, 40, 41). Germ-line transformation was performed as previously described (42). The total concentration of DNA was 100 to 110 ng/μL containing 5 to 20 ng/μL of an expression plasmid, 10 to 15 ng/μL of a fluorescent marker plasmid, and pPD49.26 as a carrier DNA.

DAG Imaging. Imaging of Downward DAG2 was performed as previously described (19).

Animals were grown with OP50 for 4 d and transferred to 100-mM conditioning plates with OP50 as described in Behavioral Tests. The worms were then washed with imaging buffer from the 100-mM conditioning plates. The imaging buffer contains 100 mM NaCl, 25 mM potassium phosphate, 1 mM $CaCl_2$, 1 mM $MgSO_4$, and 0.05% gelatin; the osmolarity was adjusted to 350 mOsm with glycerol. Subsequently, the worms were loaded into a dimethylpolysiloxane (PDMS) chip attached to inlet tubes (41). NaCl step stimulus from 100 mM to 50 mM was delivered to the nose tip of the worms by switching the solutions. Images were captured at 1 frame per second by timelapse imaging using a LEICA DMI6000B inverted microscope. For quantification, the average fluorescence intensity over 50 frames (50 s) prior to stimulation was set as F0.

To measure the basal level of DAG, young adult animals fed OP50 were placed on 5% agar pads. The animals were paralyzed with 1 mM tetramisole hydrochloride. The images were captured using the experimental setup described in the previous paragraph.

Genetic Screens for pkc-1(nj3) Suppressors and Identification of goa-1(pe3800). Mutagenesis with EMS was performed as previously described (39). The F1 progeny (150,000 worms in total) of mutagenized *pkc-1(nj3)* mutants were separated into 120 independent groups. The F2 animals (1,500 × 120 in total) were grown on NGM plates with 50 mM NaCl and placed onto the assay plates as described in *Behavioral Tests*. After 50 to 60 min, worms in the "High NaCl" area, described in Fig. 1*A*, were collected. We repeated this selection process four times and subsequently singled out a worm from each plate. Among 17 suppressor candidates obtained, only *pe3800* showed strong suppression of *pkc-1(nj3)*. *pe3800* were backcrossed five times, and then we sequenced the whole genome of *pkc-1(nj3)* and a backcrossed strain (43). A high frequency of putative EMS-induced single-nucleotide variants (G to A or C to T) was observed on the left arm of the chromosome I (0 to 8 Mb). This region had 11 missense mutations, among which we found the *goa-1* H322Y mutation. We validated H322Y as a causal mutation by a transgenic rescue experiment (Fig. 1*B*).

Statistical Analyses. All statistical tests were performed in R scripts. Welch's test was used for comparison of a pair of strains. For multiple comparisons, a one-way ANOVA followed by Dunnett's tests or Tukey's honestly significant difference tests were used. Strains conditioned with the same concentration are compared.

Data Availability. All study data are included in the article and/or *SI Appendix*. The raw dataset for all behavioral and imaging experiments and sequence information for domain-swapped transgenes are available on Figshare (DOI 10.6084/m9.figshare.17999759).

ACKNOWLEDGMENTS. We thank Asuka Miura, Masahiro Tomioka, and Yasuaki Ike for technical advice and comments on the research. Some strains (IK130 and IG277) were provided from the Caenorhabditis Genetics Center.

1. Y. Nishizuka, The role of protein kinase C in cell surface signal transduction and tumour promotion. *Nature* **308**, 693–698 (1984).
2. Y. Nishizuka, Protein kinase C and lipid signaling for sustained cellular responses. *FASEB J.* **9**, 484–496 (1995).
3. W. Y. Lu *et al.*, G-protein-coupled receptors act via protein kinase C and Src to regulate NMDA receptors. *Nat. Neurosci.* **2**, 331–338 (1999).
4. C. F. Stevens, J. M. Sullivan, Regulation of the readily releasable vesicle pool by protein kinase C. *Neuron* **21**, 885–893 (1998).
5. M.-K. Chung, A. D. Güler, M. J. Caterina, TRPV1 shows dynamic ionic selectivity during agonist stimulation. *Nat. Neurosci.* **11**, 555–564 (2008).
6. K. T. Velázquez, H. Mohammad, S. M. Sweitzer, Protein kinase C in pain: Involvement of multiple isoforms. *Pharmacol. Res.* **55**, 578–589 (2007).
7. M.-K. Sun, D. L. Alkon, *The "Memory Kinases": Roles of PKC Isoforms in Signal Processing and Memory Formation* (Elsevier Inc., ed. 1, 2014).
8. W. S. Sossin, Isoform specificity of protein kinase Cs in synaptic plasticity. *Learn. Mem.* **14**, 236–246 (2007).
9. M. A. Sutton, M. W. Bagnall, S. K. Sharma, J. Shobe, T. J. Carew, Intermediate-term memory for site-specific sensitization in aplysia is maintained by persistent activation of protein kinase C. *J. Neurosci.* **24**, 3600–3609 (2004).
10. S. Ohno, Y. Nishizuka, Protein kinase C isotypes and their specific functions: Prologue. *J. Biochem.* **132**, 509–511 (2002).
11. E. Lessmann, M. Leitges, M. Huber, A redundant role for PKC-epsilon in mast cell signaling and effector function. *Int. Immunol.* **18**, 767–773 (2006).
12. S. Carracedo, F. Sacher, G. Brandes, U. Braun, M. Leitges, Redundant role of protein kinase C delta and epsilon during mouse embryonic development. *PLoS One* **9**, e103686 (2014).
13. Y. Tabuse, Protein kinase C isotypes in *C. elegans*. *J. Biochem.* **132**, 519–522 (2002).
14. M. R. Edwards, *et al.*, PKC-2 phosphorylation of UNC-18 Ser322 in AFD neurons regulates temperature dependency of locomotion. *J. Neurosci.* **32**, 7042–7051 (2012).
15. N. Sakai, H. Ohno, M. Tomioka, Y. Iino, The intestinal TORC2 signaling pathway contributes to associative learning in *Caenorhabditis elegans*. *PLoS One* **12**, e0177900 (2017).
16. Y. Okochi, K. D. Kimura, A. Ohta, I. Mori, Diverse regulation of sensory signaling by *C. elegans* nPKC-epsilon/eta TTX-4. *EMBO J.* **24**, 2127–2137 (2005).
17. M. Tsunozaki, S. H. Chalasani, C. I. Bargmann, A behavioral switch: cGMP and PKC signaling in olfactory neurons reverses odor preference in *C. elegans*. *Neuron* **59**, 959–971 (2008).
18. H. Kunitomo *et al.*, Concentration memory-dependent synaptic plasticity of a taste circuit regulates salt concentration chemotaxis in *Caenorhabditis elegans*. *Nat. Commun.* **4**, 2210 (2013).
19. H. Ohno, N. Sakai, T. Adachi, Y. Iino, Dynamics of presynaptic diacylglycerol in a sensory neuron encode differences between past and current stimulus intensity. *Cell Rep.* **20**, 2294–2303 (2017).
20. L. Luo *et al.*, Dynamic encoding of perception, memory, and movement in a *C. elegans* chemotaxis circuit. *Neuron* **82**, 1115–1128 (2014).
21. C. Bastiani, J. Mendel, Heterotrimeric G proteins in *C. elegans*. *WormBook*, 1–25 (2006).
22. T. Adachi *et al.*, Reversal of salt preference is directed by the insulin/PI3K and Gq/PKC signaling in *Caenorhabditis elegans*. *Genetics* **186**, 1309–1319 (2010).
23. P. Tewson *et al.*, Simultaneous detection of Ca2+ and diacylglycerol signaling in living cells. *PLoS One* **7**, e42791 (2012).
24. T. Sano, Y. Tabuse, K. Nishiwaki, J. Miwa, The tpa-1 gene of *Caenorhabditis elegans* encodes two proteins similar to Ca(2+)-independent protein kinase Cs: Evidence by complete genomic and complementary DNA sequences of the tpa-1 gene. *J. Mol. Biol.* **251**, 477–485 (1995).
25. Y. Tabuse, K. Nishiwaki, J. Miwa, Mutations in a protein kinase C homolog confer phorbol ester resistance on *Caenorhabditis elegans*. *Science* **243**, 1713–1716 (1989).
26. J. Miwa, Y. Tabuse, M. Furusawa, H. Yamasaki, Tumor promoters specifically and reversibly disturb development and behavior of *Caenorhabditis elegans*. *J. Cancer Res. Clin. Oncol.* **104**, 81–87 (1982).
27. R. N. Arey, G. M. Stein, R. Kaletsky, A. Kauffman, C. T. Murphy, Activation of $G_{\alpha q}$ signaling enhances memory consolidation and slows cognitive decline. *Neuron* **98**, 562–574.e5 (2018).

NEUROSCIENCE

28. J. Gong *et al.*, A Cold-sensing receptor encoded by a glutamate receptor gene. *Cell* **178**, 1375–1386.e11 (2019).
29. M. Ren, H. Feng, Y. Fu, M. Land, C. S. Rubin, Protein kinase D is an essential regulator of *C. elegans* innate immunity. *Immunity* **30**, 521–532 (2009).
30. K. S. Kindt *et al.*, Dopamine mediates context-dependent modulation of sensory plasticity in *C. elegans*. *Neuron* **55**, 662–676 (2007).
31. D. Ventimiglia, "*A comparative study of sensory neuron synaptic activity and the role of presynaptic diversity, specificity, and regulation in Caenorhabitis elegans,* " PhD dissertation, Rockfeller University, New York, NY (2017).
32. H. Mischak *et al.*, Phorbol ester-induced myeloid differentiation is mediated by protein kinase C-alpha and -delta and not by protein kinase C-beta II, -epsilon, -zeta, and -eta. *J. Biol. Chem.* **268**, 20110–20115 (1993).
33. E. N. Churchill, D. Mochly-Rosen, The roles of PKCdelta and epsilon isoenzymes in the regulation of myocardial ischaemia/reperfusion injury. *Biochem. Soc. Trans.* **35**, 1040–1042 (2007).
34. W. F. Ochoa *et al.*, Structure of the C2 domain from novel protein kinase Cε. A membrane binding model for Ca2+-independent C2 domains. *J. Mol. Biol.* **311**, 837–849 (2001).
35. C. A. Farah, W. S. Sossin, The role of C2 domains in PKC signaling. *Adv. Exp. Med. Biol.* **740**, 663–683 (2012).
36. C. H. Benes *et al.*, The C2 domain of PKCdelta is a phosphotyrosine binding domain. *Cell* **121**, 271–280 (2005).
37. A. Pascale *et al.*, Functional impairment in protein kinase C by RACK1 (receptor for activated C kinase 1) deficiency in aged rat brain cortex. *J. Neurochem.* **67**, 2471–2477 (1996).
38. J. Hongpaisan, C. Xu, A. Sen, T. J. Nelson, D. L. Alkon, PKC activation during training restores mushroom spine synapses and memory in the aged rat. *Neurobiol. Dis.* **55**, 44–62 (2013).
39. S. Brenner, The genetics of *Caenorhabditis elegans*. *Genetics* **77**, 71–94 (1974).
40. M. Matsuki, H. Kunitomo, Y. Iino, Goalpha regulates olfactory adaptation by antagonizing Gqalpha-DAG signaling in *Caenorhabditis elegans*. *Proc. Natl. Acad. Sci. U.S.A.* **103**, 1112–1117 (2006).
41. N. Chronis, M. Zimmer, C. I. Bargmann, Microfluidics for in vivo imaging of neuronal and behavioral activity in *Caenorhabditis elegans*. *Nat. Methods* **4**, 727–731 (2007).
42. C. C. Mello, J. M. Kramer, D. Stinchcomb, V. Ambros, Efficient gene transfer in *C. elegans*: Extrachromosomal maintenance and integration of transforming sequences. *EMBO J.* **10**, 3959–3970 (1991).
43. S. Zuryn, S. Le Gras, K. Jamet, S. Jarriault, A strategy for direct mapping and identification of mutations by whole-genome sequencing. *Genetics* **186**, 427–430 (2010).